

Supporting Information for:

Tracing the ‘9th Sulfur’ of the Nitrogenase Cofactor via a Semi-Synthetic Approach

Kazuki Tanifuji,¹ Chi Chung Lee,¹ Nathaniel S. Sickerman,¹ Kazuyuki Tatsumi,² Yasuhiro Ohki,² Yilin Hu,^{1,*} and Markus W. Ribbe^{1,3,*}

¹ Department of Molecular Biology and Biochemistry, University of California, Irvine, California 92697-3900

² Department of Chemistry, Graduate School of Science and Research Center for Materials Science, Nagoya University, Furo-cho, Chikusa-ku, Nagoya 464-8602, Japan

³ Department of Chemistry, University of California, Irvine, California 92697-2025

*Correspondence should be addressed to mribbe@uci.edu or yilinh@uci.edu.

Table of Contents

Supplementary Methods

Cell Growth and Protein Purification	3
EPR Analysis	4
ICP-OES Analysis	4
Activity Assays of NifH	5
SAM Cleavage Assays	5
Cluster Maturation Assays	6
Acid Quench Experiments	7

Supplementary References	8
--------------------------	---

Supplementary Figures

Supplementary Figure 1	10
Supplementary Figure 2	10
Supplementary Figure 3	11
Supplementary Figure 4	11
Supplementary Figure 5	12
Supplementary Figure 6	13

Supplementary Methods

Unless otherwise specified, all chemicals were purchased from Sigma-Aldrich (St. Louis, MO) and Thermo Fisher Scientific (Waltham, MA). ^{35}S -labelled sodium sulfite ($\text{Na}_2^{35}\text{SO}_3$) was purchased from Moravek, Inc (Brea, CA). For chemical synthesis, all reactions were performed under an N_2 atmosphere using Schlenk techniques and a glove box operating at <1 ppm H_2O and O_2 . Electronic absorption was measured with an Evolution 260 BIO UV-visible spectrometer (Thermo Fisher) using a 1 cm cuvette. All solvents were purified before use by passing through columns of activated alumina and a supported copper catalyst. $[\text{PPh}_4]_2[\text{Fe}_4\text{S}_4(\text{SEt})_4]$ was prepared as described elsewhere¹ and used as the precursor for the synthesis of $[\text{PPh}_4]_2[\text{Fe}_4\text{S}_4(\text{SCH}_2\text{CH}_2\text{OH})_4]$ (designated $[\text{PPh}_4]_2[\text{Fe}_4\text{S}_4]^{\text{Syn}}$) using a protocol slightly modified from a previously described procedure.² 2-Mercaptoethanol (BME) was degassed by three freeze-pump-thaw cycles prior to use. For biochemical experiments, unless otherwise noted, all manipulations were performed under an Ar atmosphere using Schlenk techniques and a glove box operating at <3 ppm O_2 . Aqueous solutions of europium(II) diethylenetriaminepentaacetic acid (Eu^{II} -DTPA) or europium(II) ethyleneglycol-bis(2-aminomethylether)-*N,N,N',N'*-tetraacetic acid (Eu^{II} -EGTA) were prepared immediately before use as described earlier.³

Cell Growth and Protein Purification. An *Escherichia coli* strain (YM114EE) expressing His-tagged NifB of *Methanosarcina acetivorans* (*MaNifB*) was grown and harvested as described elsewhere.⁴ Published methods were used to purify *MaNifB*.⁴ *Azotobacter vinelandii* strains (YM9A, DJ1143 and DJ1141) expressing His-tagged $\Delta nifB$ NifEN (designated NifEN^{apo}), His-tagged $\Delta nifB$ NifDK (designated NifDK^{apo}), His-tagged wildtype NifDK (designated NifDK^{holo}) and non-tagged wildtype NifH (designated NifH^{holo}), respectively, were grown and harvested as described earlier.⁵⁻⁸ Published methods were used

to purify NifEN^{apo}, NifDK^{apo}, NifDK^{holo} and NifH^{holo}.⁵⁻⁸

EPR Analysis. The EPR samples were prepared in a Vacuum Atmospheres glove box and flash frozen in liquid nitrogen prior to analysis. The DT-reduced samples contained 2 mM DT, 50 mM Tris-HCl (pH 8.0), 500 mM NaCl and 10% (v/v) glycerol. The indigo disulfonate (IDS)-oxidized samples were prepared by incubating the DT-reduced samples with excess IDS for 5 min, followed by removal of excess IDS using a Sephadex G-25 desalting column. The super-reduced samples were prepared by incubating the DT-reduced sample with excess Eu^{II}-DTPA for 20 min, followed by removal of excess Eu^{II}-DTPA using a Sephadex G-25 desalting column. The NifH samples contained either no nucleotide or 5 mM ATP or ADP; whereas the *MaNifB* samples contained either no SAM or 10 mM SAM. The DT-free *MaNifB* samples contained 2 mM Eu^{II}-EGTA and either no additive or 10 mM SAM with or without 2 mM sodium sulfite (Na₂SO₃). EPR spectra were recorded by an ESP 300 E_z spectrophotometer (Bruker) interfaced with an ESR-9002 liquid-helium continuous-flow cryostat (Oxford Instruments) using a microwave power of 50 mW, a gain of 5×10⁴, a modulation frequency of 100 kHz, and a modulation amplitude of 5 G. Five scans were recorded for each EPR sample at a temperature of 10 K and a microwave frequency of 9.62 GHz (*see* Fig. 2b; Fig. 3c, d; Supplementary Fig. 1).

Inductively Coupled Plasma Optical Emission Spectroscopy (ICP-OES) Analysis. The metal contents of NifH^{holo}, NifH^{apo}, and NifH^[Fe₄S₄] were determined by inductively coupled plasma optical emission spectroscopy (ICP-OES) using a Thermo Scientific iCAP7000 (Thermo Electron North America LLC, Madison, WI). Stock solution of Fe (1000 mg·L⁻¹) was diluted to make standard solutions for calibration. Each protein sample was mixed with 100 μL concentrated H₂SO₄ and 100 μL concentrated HNO₃, and subsequently refluxed at

250°C for 30 min. This procedure was repeated until the solution became colorless, followed by cooling of the solution to room temperature and dilution of this solution with a 2% (w/w) HNO₃ solution to a total volume of 6 mL for ICP-OES measurement.

Activity Assays of NifH. Activity assays of the NifH samples (*see* Supplementary Fig. 1) were carried out as described earlier.⁹ The products of the reactions were analyzed as described previously.⁸⁻¹⁰

SAM Cleavage Assays. The SAM cleavage assays contained, in a total volume of 0.5 ml, 25 mM Tris-HCl (pH 8.0), 2 mM DT, 5% (v/v) glycerol, 8 nmol *MaNifB*^{apo} or *MaNifB*^[Fe₄S₄], and 8 nmol SAM (*see* Fig. 2a). The DT-free assays contained the same components except for the substitution of 0.3 mM Eu^{II}-EGTA and 8 nmol DT-free *MaNifB*^[Fe₄S₄], respectively, for DT and the DT-containing *MaNifB* sample, with or without addition of 0.5 mM Na₂SO₃ (*see* Fig. 3b). Assays were incubated at 25°C for 30 min with intermittent mixing, before being terminated by filtration with Amicon Ultra 30,000 MWCO centrifugal filters. Trifluoroacetic acid was supplemented at a concentration of 0.14% (w/w) to the filtered samples before the samples were analyzed using a Thermo Scientific Dionex Ultimate 3000 UHPLC system with an Acclaim 120 C18 column (4.6×100 mm, 5-μm particle size). The column was equilibrated with 98% buffer A (50 mM KH₂PO₄, pH 6.6) and 2% buffer B (100% methanol). Following each 100-μl injection of sample, a linear gradient of 60–95% buffer B was applied over 20 min, followed by 8 min of isocratic flow with 95% buffer B and a linear gradient of 95–2% buffer B over 3 min. The buffer flow rate was 0.5 ml/min throughout each run and the column was maintained at 30°C. The column was then equilibrated for 5 min with 2% buffer B before subsequent sample injections. The elution of SAM, *S*-adenosyl-L-homocysteine (SAH), and 5'-deoxyadenosine (5'-dAH) were monitored by UV absorption at 254 nm, and

the respective compounds were identified by comparing their retention times with those of the known standards.

Cluster Maturation Assays. Cluster maturation assays were conducted using the SAM-treated *MaNifB*^[Fe₄S₄] as an L-cluster source in the presence or absence of DT. The DT-containing assays (*see* Fig. 2c) contained, in a total volume of 1 mL, 84 nmol *MaNifB*^[Fe₄S₄], 10 nmol NifEN^{apo}, 22 nmol NifH^{holo}, 2.0 nmol NifDK^{apo}, 20 mM DT, 5 mM SAM, 0.5 mM homocitrate, 0.25 mM sodium molybdate (Na₂MoO₄), 0.8 mM Na₂ATP, 1.7 mM MgCl₂, 10 mM creatine phosphate, 8 units of creatine phosphokinase, and 50 mM Tris-HCl (pH 8.0). This mixture was incubated at 30°C for 30 min before it was examined for enzymatic activities as described previously.⁴ The DT-free assay (*see* Fig. 3e) was initiated with incubation of 42 nmol DT-free *MaNifB*^[Fe₄S₄] with 2 mM Na₂SO₃, 2 mM Eu^{II}-EGTA, 5 mM SAM, 50 mM Tris-HCl (pH 8.0) and 10% (v/v) glycerol in a total volume of 450 μL at room temperature for 5 min. The “-SAM, -SO₃²⁻” or “+SAM, -SO₃²⁻” control (*see* Fig. 3e) contained the same components as those of the DT-free assay except for the absence of both SAM and Na₂SO₃, or the absence of Na₂SO₃ alone; whereas the “no sulfur” control and the “sulfate”, “sulfide” and “DT” samples (*see* Supplementary Fig. 2) contained the same components as those of the DT-free assay except for the substitution of no additive, 2 mM MgSO₄, 2 mM Na₂S, and 2 mM DT, respectively, for Na₂SO₃. Following the incubation, the mixture was combined with a 900-μL mixture containing 10 nmol NifEN^{apo}, 22 nmol NifH^{holo}, 2.0 nmol NifDK^{apo}, 2 mM Eu^{II}-EGTA, 5 mM SAM, 0.5 mM homocitrate, 0.25 mM Na₂MoO₄, 0.8 mM Na₂ATP, 1.7 mM MgCl₂, 10 mM creatine phosphate, 8 units of creatine phosphokinase, and 50 mM Tris-HCl (pH 8.0). This reaction mixture was incubated at 30°C for 30 min, terminated with addition of 0.4 mM ammonium tetrathiomolybdate [(NH₄)₂MoS₄], and examined for the enzymatic activity under 10% C₂H₂.

To confirm the generation of L-cluster on *Ma*NifB^[Fe₄S₄] in the presence of Na₂SO₃ (*see* Fig. 3a, *right*), the NifB-bound cluster species was extracted from a 120- μ L mixture containing 67 nmol DT-free *Ma*NifB^[Fe₄S₄], 2 mM Na₂SO₃, 2 mM Eu^{II}-EGTA, 5 mM SAM, 10% (v/v) glycerol and 50 mM Tris-HCl (pH 8.0) into a 50- μ L *N*-methylformamide (NMF) solution containing 2.5 mM 1,4-benzenedithiol using a protocol adapted from a previously described procedure.¹¹ The same protocol was used to prepare an NMF extract from a “-SAM, +SO₃²⁻” control containing the same components except for the absence of SAM (*see* Fig. 3a, *right*). The cluster extract was then mixed with 10 nmol NifEN^{apo} in 1 mL buffer containing 2 mM DT and 50 mM Tris-HCl (pH 8.0), concentrated to 450 μ L, and mixed with 22 nmol NifH^{holo} and 2 nmol NifDK^{apo} in 900 μ L buffer containing 20 mM DT, 0.5 mM homocitrate, 0.25 mM Na₂MoO₄, 0.8 mM Na₂ATP, 1.7 mM MgCl₂, 10 mM creatine phosphate, 8 units of creatine phosphokinase, and 50 mM Tris-HCl (pH 8.0). This reaction mixture was incubated at 30°C for 30 min and examined for enzymatic activities as described earlier.⁴

Acid Quench Experiments. A published method was adapted for the *Ma*NifB^[Fe₄S₄]-dependent formation of methanethiol.¹² These assays were carried out under 100% Ar in 400- μ L sealed glass vials. Each assay contained, in a total volume of 100 μ L, 50 mM 10 nmol DT-free NifB^[Fe₄S₄], 2 mM Eu^{II}-EGTA, 200 nmol SAM, 200 nmol or no Na₂SO₃, 10% (v/v) glycerol, 50 mM Tris-HCl (pH 8.0) (*see* Supplementary Fig. 3). The reaction mixture was incubated at 25°C for 30 min before being quenched by addition of 25 μ L HCl (1 M). To detect the volatile methanethiol (boiling point: 6°C), the acid-quenched sample was incubated at 60°C for 15 min and equilibrated at room temperature for 15 min before 100 μ L headspace of the assay vial was injected onto an Rxi-1ms column (0.32 mm diameter, 30 m length, 4 μ m film thickness; Restek) in a TRACE 1300 gas chromatograph equipped with an ISQ-QD single

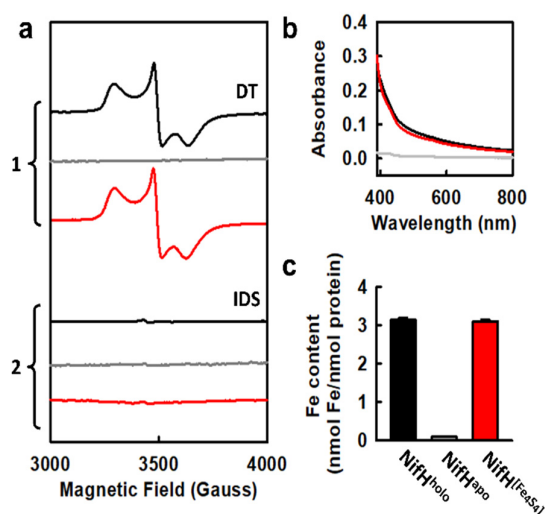
quadrupole mass spectrometer (Thermo Scientific). The column was held at 30°C for 8 min, heated up to 200°C at 40°C/min, held at 200°C for 1min, and cooled down to 30°C. The gas chromatograph-mass spectrometry (GC-MS) full scan spectra were generated from a mass range between $m/z = 43.00$ and $m/z = 55.00$. Total ion chromatograms were generated under SIM condition with $m/z = 47.00$. To determine the amounts of methanethiol in samples, aqueous solutions of sodium methanethiolate were prepared at 0, 40, 80, and 160 μM and quenched by the same procedure applied to the samples. Approximately 40% (4 nmol) of the theoretical yield of methanethiol was detected in the assay.

Supplementary References

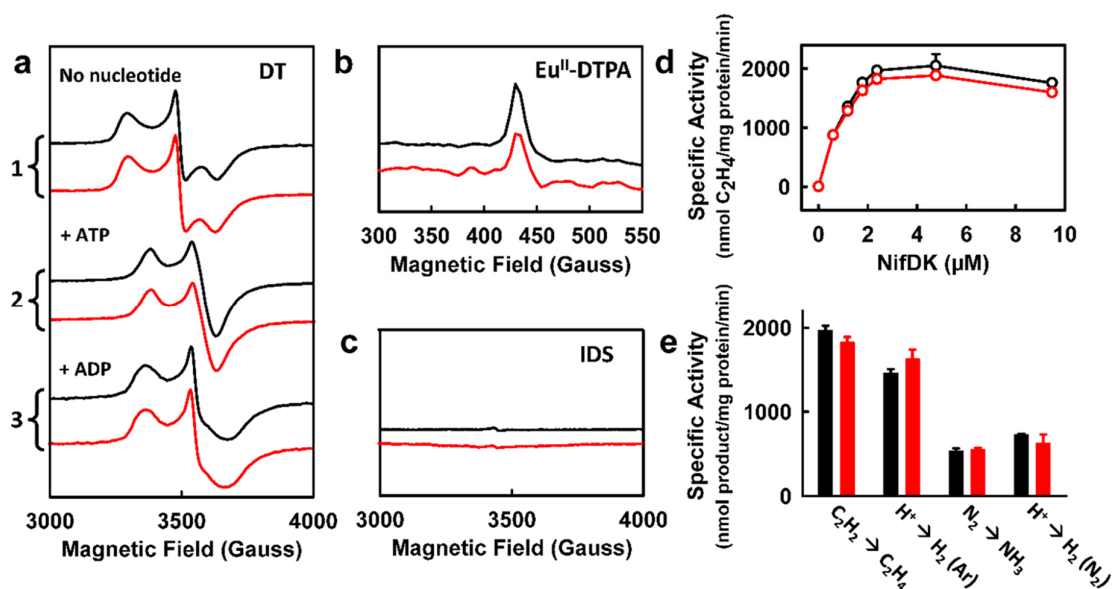
1. Averill, B. A., Herskovitz, T., Holm, R. H. & Ibers, J. A. Synthetic analogs of the active sites of iron-sulfur proteins. II. Synthesis and structure of the tetra(mercapto- μ_3 -sulfido-iron) clusters, $(\text{Fe}_4\text{S}_4(\text{SR})_4)^{2-}$. *J. Am. Chem. Soc.* **95**, 3523–3534 (1973).
2. Barclay, J. E., Davies, S. C., Evans, D. J. & Hughes, D. L. Lattice effects in the Mössbauer spectra of salts of $[\text{Fe}_4\text{S}_4\{\text{S}(\text{CH}_2)_n\text{OH}\}_4]^{2-}$. Crystal structures of $[\text{PPh}_4]_2[\text{Fe}_4\text{S}_4\{\text{S}(\text{CH}_2)_n\text{OH}\}_4]$ ($n=2, 3$ and 4). *Inorg. Chim. Acta.* **291**, 101–108 (1999).
3. Vincent, K. A. *et al.* Instantaneous, stoichiometric generation of powerfully reducing states of protein active sites using Eu(II) and polyaminocarboxylate ligands. *Chem. Commun.* **2003**, 2590–2591 (2003).
4. Fay, A. W., Wiig, J. A., Lee, C. C. & Hu, Y. Identification and characterization of functional homologs of nitrogenase cofactor biosynthesis protein NifB from methanogens. *Proc. Nat. Acad. Sci. U.S.A.* **112**, 14829–14833 (2015).
5. Hu, Y., Fay, A. W. & Ribbe, M. W. Identification of a nitrogenase FeMo cofactor precursor on NifEN complex. *Proc. Natl. Acad. Sci. U.S.A.* **102**, 3236–3241 (2005).
6. Ribbe, M. W., Hu, Y., Guo, M., Schmid, B. & Burgess, B. K. The FeMoco-deficient MoFe protein produced by a *nifH* deletion strain of *Azotobacter vinelandii* shows unusual P-cluster features. *J. Biol. Chem.* **277**, 23469–23476 (2002).
7. Christiansen, I. J., Goodwin, P. J., Lanzilotta, W. N., Seefeldt, L. C. & Dean, D. R.

- Catalytic and biophysical properties of a nitrogenase Apo-MoFe protein produced by a *nifB*-deletion mutant of *Azotobacter vinelandii*. *Biochemistry* **37**, 12611–12623 (1998).
8. Burgess, B. K., Jacobs, D. B. & Stiefel, E. I. Large-scale purification of high activity *Azotobacter vinelandii* nitrogenase. *Biochim. Biophys. Acta.* **614**, 196–209 (1980).
 9. Ribbe, M. W., Bursey, E. H. & Burgess, B. K. Identification of an Fe protein residue (Glu146) of *Azotobacter vinelandii* nitrogenase that is specifically involved in FeMo cofactor insertion. *J. Biol. Chem.* **275**, 17631–17638 (2000).
 10. Gavini, N. & Burgess, B. K. FeMo cofactor synthesis by a *nifH* mutant with altered MgATP reactivity. *J. Biol. Chem.* **267**, 21179–21186 (1992).
 11. Wiig, J. A., Hu, Y., Lee, C. C. & Ribbe, M. W. Radical SAM-dependent carbon insertion into the nitrogenase M-cluster. *Science* **337**, 1672–1675 (2012).
 12. Wiig, J. A., Hu, Y. & Ribbe, M. W. Refining the pathway of carbide insertion into the nitrogenase M-cluster. *Nat. Commun.* **6**, 8034 (2015).

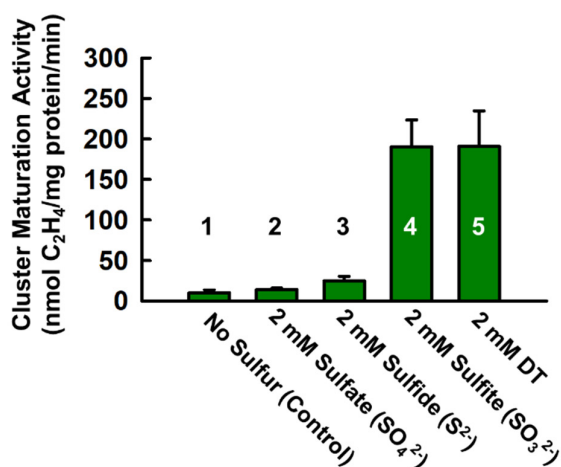
Supplementary Figures



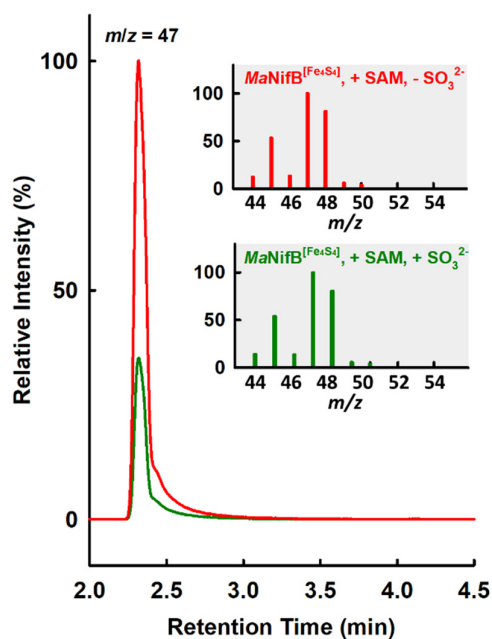
Supplementary Figure 1. Characterization of NifH^{apo} reconstitution. (a) EPR spectra of NifH^{holo} (black), NifH^{apo} (gray) and NifH^[Fe₄S₄] (red) in the DT-reduced (1) and IDS-oxidized (2) states. (b) Visible absorption spectra of NifH^{holo} (black), NifH^{apo} (gray) and NifH^[Fe₄S₄] (red). (c) Fe content of NifH^{holo} (black), NifH^{apo} (gray) and NifH^[Fe₄S₄] (red) as determined by ICP-OES.



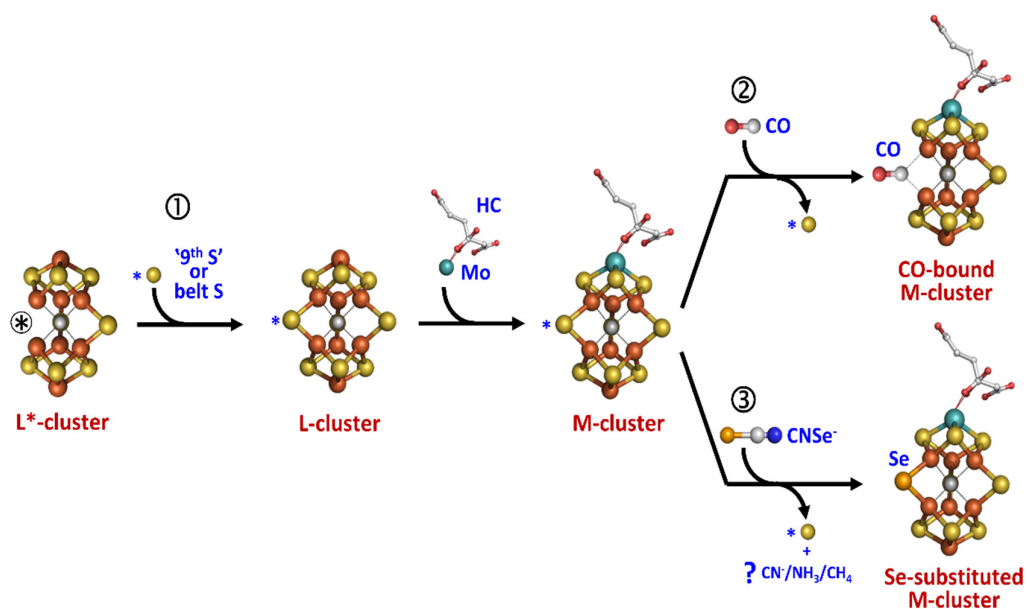
Supplementary Figure 2. Characterization of NifH^[Fe₄S₄]. (a-c) EPR spectra of NifH^{holo} (black) and NifH^[Fe₄S₄] (red) in the presence of DT (a), Eu^{II}-DTPA (b) and IDS (c). DT-reduce samples contained no nucleotide (a, 1), ATP (a, 2) or ADP (a, 3). (d) Catalytic profiles of NifH^{holo} (black) and NifH^[Fe₄S₄] (red) titrated with increasing amounts of NifDK^{holo}. (e) Activities of C₂H₂-, H⁺- and N₂-reduction by NifDK^{holo} when combined with NifH^{holo} (black) or NifH^[Fe₄S₄] (red).



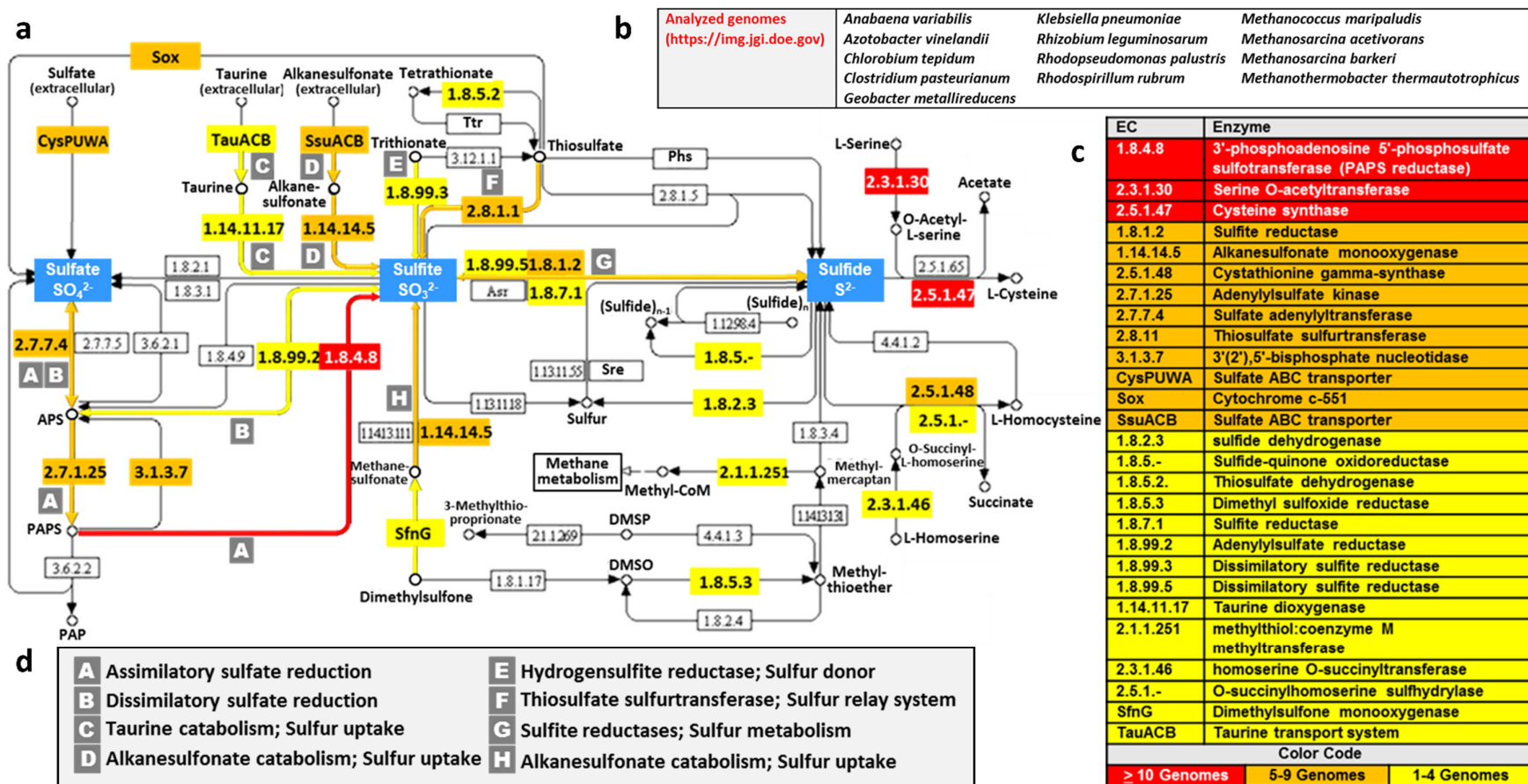
Supplementary Figure 3. Identification of the origin of the ‘9th S’. Activities of substrate reduction by *MaNifB*^[Fe₄S₄] treated with (1) no sulfur, (2) 2 mM MgSO₄, (3) 2 mM Na₂S, (4) 2 mM Na₂SO₃, and (5) 2 mM DT, after maturation and transfer of clusters to NifDK. Assays 1-4 were conducted in 2 mM Eu^{II}-EGTA, and assay 5 contained 2 mM DT.



Supplementary Figure 4. Formation of methanethiol by acid-quenched *MaNifB*^[Fe₄S₄]. GC-MS full scans (inset) and SIM ($m/z=47$) analyses of acid-quenched incubation mixtures containing *MaNifB*^[Fe₄S₄] and SAM in the absence (red) or presence (green) of SO₃²⁻. Both assays contained 2 mM Eu^{II}-EGTA. The acid-quenched product was identified as methanethiol based on its GC-MS retention time and fragmentation pattern.



Supplementary Figure 5. Fate of the ‘9th S’ in assembly and catalysis. Comparison of the insertion of the ‘9th S’ as a belt S during M-cluster assembly ① with the replacement of a belt S of the M-cluster by CO ② or Se ③ under turnover conditions. The apparent analogy between these events suggests the possibility to specifically label the ‘9th S’ for tackling the reactive Fe sites coordinated by this atom during catalysis. The encircled black asterisk (*) in the L*-cluster denotes potential ligand binding site. The blue asterisks in the L- and M-clusters denote the incorporated ‘9th S’.



Supplementary Figure 6. Analysis of sulfur metabolism of selected nitrogen fixing microbes. (a) Pathways of sulfur metabolism in the cell, where sulfate, sulfite and sulfide are three major metabolites. The map of sulfur metabolism was rendered at JGI (<http://img.jgi.doe.gov>). (b) 13 nitrogen-fixing (diazotrophic) organisms analyzed for genes encoding enzymes involved in sulfur metabolism. (c) Genes encoding sulfur-metabolizing enzymes identified in ≥ 10 (red), 5-9 (orange) or 1-4 (yellow) of the 13 selected genomes of diazotrophic organisms. (d) Sulfite-generating pathways utilizing enzymes encoded by genes identified in the 13 selected genomes of diazotrophic organisms. Note that the sulfite-generating pathway involving the PAPS reductase (a, red arrow) is the most predominant among the 13 selected organisms based on genomic analyses.